JBUON 2021; 26(4): 1333-1339
ISSN: 1107-0625, online ISSN: 2241-6293 • www.jbuon.com
Email: editorial_office@jbuon.com

ORIGINAL ARTICLE

FBXL19-AS1 aggravates the progression of hepatocellular cancer by downregulating KLF2

Yudan Chen, Linglin Yang

Department of Oncology, the Affiliated Hospital of Southwest Medical University

Summary

Purpose: *To uncover the role of FBXL19-AS1 in aggravating the progression of hepatocellular cancer (HCC) by downregulating kruppel-likefactor2 (KLF2).*

Methods: *FBXL19-AS1 level in HCC tissues and adjacent normal tissues were firstly determined. Its level in HCC with different tumor sizes (≤ 5 cm or >5 cm) and different tumor stages (stage I-II or III-IV) was examined as well. Subcellular distribution of FBXL19-AS1 was detected. The regulatory effect of FBXL19-AS1 on viability, apoptosis and cell cycle progression of HCC cells was assessed. RNA immunoprecipitation (RIP) assay was conducted to explore the interaction between FBXL19-AS1 with EZH2 and SUZ12. Moreover, chromatin immunoprecipitation (ChIP) assay was carried out to identify the recruitment ability of FBXL19-AS1 on EZH2 and H3K27me3. Finally, the potential role of KLF2 in FBXL19-AS1-mediated HCC proliferation was investigated.*

Results: *FBXL19-AS1 was highly expressed in HCC tissues, especially in those larger than 5 cm in tumor size and worse tumor stage. FBXL19-AS1 was mainly distributed in nucleus and interacted with EZH2 and SUZ12. Knockdown of FBXL19-AS1 suppressed proliferation, cell cycle progression and induced apoptosis of HCC cells. Moreover, silence of FBXL19-AS1 attenuated the recruitment ability of EZH2 on KLF2. Knockdown of KLF2 reversed the regulatory effect of FBXL19-AS1 on proliferative ability of HCC cells.*

Conclusions: *Long non-coding RNA (lncRNA) FBXL19-AS1 is upregulated in HCC. It accelerates proliferative ability, cell cycle progression and suppresses apoptosis of tumor cells through interacting with KLF2, thus aggravating the progression of HCC.*

Key words: *hepatocellular cancer (HCC); FBXL19-AS1; KLF2*

Introduction

Hepatocellular cancer (HCC) is a prevalent tumor ranking the third in the mortality of malignancies [1]. Most of HCC patients are already in advanced stage at diagnosis. Only 20% of HCC patients could be treated by surgery, radiofrequency ablation and liver transplantation [2]. The efficacy of surgical treatment for HCC is not satisfactory owing to tumor recurrence and metastasis. The postoperative 5-year survival of HCC is about 65-75% [3,4]. Recurrent HCC extremely endangers patient lives. Hence, development of diagnostic and therapeutic targets for HCC is of great significance.

Long non-coding RNA (lncRNA) is a kind of ncRNA with more than 200 nt in length and it is mainly located in the nucleus or cytoplasm [5]. In 2002, Okazaki et al [6] first discovered lncRNA in the large-scale sequencing of mouse transcriptome based on functional annotation of 60,770 full-length complementary deoxyribose nucleic acids (cDNAs). LncRNAs exert diverse functions in regulating cellular behaviors [7]. Moreover, lncRNAs are abnormally expressed in many tumor diseases [8-10]. Zhang et al [11] reported that lncRNA H19 is closely related to prognosis of liver cancer, which

Corresponding author: Linglin Yang, MD. Department of Oncology, the Affiliated Hospital of Southwest Medical University, 25 Taiping Street, Jiangyang District, Luzhou, Sichuan 646000, China.
Tel: +860830-3165120; Email: yanglinglin2003@qq.com
Received: 15/05/2021; Accepted: 08/06/2021

could accelerate invasion and metastasis of liver cancer cells. A previous research indicated that FBXL19-AS1 exerts a carcinogenic role in colorectal cancer [12]. However, the biological function and molecular mechanism of lncRNA FBXL19-AS1 in HCC are still unclear.

The kruppel-likefactor (KLF) transcription factor family has a Cys2/His2 zinc finger domain that mediates cell differentiation and proliferation [13]. KLF2, located on chromosome 19p13.1, is a member of the KLFs family. It was first discovered in human lung tissues [14]. Recent studies have reported that LINC00460 can promote the development of colorectal cancer by regulating the expression of KLF2 [15]. This study explored the role of FBXL19-AS1 and KLF2 in the progression of HCC. We aim to provide potential targets for HCC diagnosis and treatment.

Methods

Subjects

HCC tissues and adjacent normal tissues were harvested from 60 HCC patients. Clinical indexes and follow-up data of enrolled HCC patients were collected. None of these patients were preoperatively treated. This study was approved by the Medical Ethics Committee of our hospital (15-SC-XNYK-04329) and informed consent was provided from each subject.

Cell culture and transfection

Normal liver cell line and HCC cell lines were cultured in Dulbecco's Modified Eagle Medium (DMEM) (Gibco, Rockville, MD, USA) containing 10% fetal bovine serum (FBS) (Gibco, Rockville, MD, USA) and 1% penicillin-streptomycin in a 5% CO_2 incubator at 37°C. Cells in logarithmic growth phase were selected for transfection using Lipofectamine 2000 (Invitrogen, Carlsbad, CA, USA). Fresh medium was replaced at 24 h. Sequences of transfection vectors were as follows: sh-FBXL19-AS1: 5'-CCGGCCTCCCTAAGTGTTGGGATTACTCGAGTAATCCCAACACTTAGGGAGGTTTTTTG-3'; sh-FBXL19-AS1: 5'-CCGGGCATTTAATTTGGCATAGCAACTCGAGTTGCTATGCCAAATTAAATGCTTTTTTG-3'; sh-NC: forward, 5'-CCGGTTTCTCCGAACGTGTCACGTCTCGAGACGTGACACGTTCGGAGAATTTTTG-3' and reverse, 5'-AATTCAAAAAGTTCTCCGAACGTGTCACGTCTCGAGACGTGACACGTTCGGAGAA-3'; sh-EZH2: forward, 5'-AGAGGTACCG-GACGAAGAATAATCATGG-3' and reverse, 5'-TAGCTCGAGGGTAGCAGATGTAAGG-3'; sh-KLF2: forward 5'-GATCCGCGCACCCACGACGACCTCAATTCAAGAGATTGAGGTCGTCGTCGGTGCCGTTTTTTC-3' and reverse 5'-AATTGAAAAAACGGCACCGACGACGACCTCAATCTCTTGAATTGAGGTCGTCGTCGGTGCCGCG-3'.

Quantitative real-time polymerase chain reaction (qRT-PCR)

RNA extraction was performed using TRIzol method (Invitrogen, Carlsbad, CA, USA). The extracted RNA was quantified and reversely transcribed into cDNA, followed by PCR using SYBR Green method. Primer sequences were as follows: FBXL19-AS1: 5'-GGTACAACTACGGATATGA-3' (forward) and 5'-TACGTCTCGACCATTACGCA-3' (reverse); Glyceraldheyde 3-phosphate dehydrogenase (GAPDH): 5'-GAAGGTGAAGGTCGGAGTC-3' (forward) and 5'-GAAGATGGTGAT GGGATTTC-3' (reverse).

Cell counting kit-8 (CCK-8)

Cells were seeded in 96-well plates with 3×10^3 cells per well. Absorbance (A) at 450 nm was recorded at the appointed time points using the CCK-8 kit (Dojindo Laboratories, Kumamoto, Japan) for depicting the viability curve.

Apoptosis determination

Cells were prepared for single-cell suspension with 4×10^5 cells/mL. Cells were double-stained with 5 μL of Annexin V and 5 μL of fluorescein isothiocyanate (FITC) in the dark for 10 min. Apoptotic rate was finally determined using flow cytometry (Partec AG, Arlesheim, Switzerland).

Cell cycle detection

Cells were seeded in 6-well plates with 1×10^5 cells/mL and subjected to serum starvation for 12 h. Cells were incubated with 25 or 50 μmol/L Andro, and 0.1% dimethyl sulfoxide (DMSO) (Sigma-Aldrich, St. Louis, MO, USA) as negative control for 12, 24 and 48 h. Subsequently, cells were collected and centrifuged at 1000 r/min for 5 min. The precipitate was washed with phosphate buffered saline (PBS) once, suspended in 200 μL of PBS and fixed in pre-cooled 75% ethanol for 12 h. Cells were incubated with 100 μL propidium iodide and 100 μL RNA enzyme. Cell cycle was detected using flow cytometry.

5-Ethynyl-2'- deoxyuridine (EdU) assay

Cells were seeded in 96-well plates with 300 cells per well. Cells were labeled with 50 μmol/L EdU (Sigma-Aldrich, St. Louis, MO, USA) at 37°C for 2 h. After 30-min fixation in 4% paraformaldehyde, cells were incubated with PBS containing 0.5% Triton-100 for 20 min. After washing with PBS containing 3% bovine serum albumin (BSA), 100 μL of dying solution was applied per well for 1-h incubation in the dark and cells were counter-stained with Hoechst 33342 for 30 min. EdU-positive cells were captured under a microscope (magnification 100×).

Western blot

Total protein was extracted from cells or tissues using radioimmunoprecipitation assay (RIPA) (Beyotime, Shanghai, China) and loaded for electrophoresis. After transferring on a polyvinylidene fluoride (PVDF) membranes (Millipore, Billerica, MA, USA), it was blocked in 5% skim milk for 2 h, incubated with primary antibodies at 4°C overnight and secondary antibodies for 2 h. Bands were exposed by electrochemiluminescence (ECL) and analyzed by Image-Pro Plus (Silver Springs, MD, USA).

Determination of subcellular distribution

Cytoplasmic and nuclear RNAs were extracted using the PARIS kit (Invitrogen, Carlsbad, CA, USA) and subjected to qRT-PCR. U6 was the internal reference of nucleus and GAPDH was that of cytoplasm.

RNA immunoprecipitation (RIP)

Cells were treated according to the procedures of Millipore (Billerica, MA, USA) Magna RIPTM RNA-Binding Protein Immunoprecipitation Kit. Cell lysate was incubated with anti-EZH2, anti-SUZ12 or IgG antibody at 4°C for 6 h. A protein-RNA complex was captured and digested with 0.5 mg/ml proteinase K containing 0.1% SDS to extract RNA. The magnetic beads were repeatedly washed with RIP washing buffer to remove non-specific adsorption as much as possible. Finally, the extracted RNA was subjected to mRNA level determination using qRT-PCR.

Chromatin immunoprecipitation (ChIP)

Cells were subjected to 10-min cross-link with 1% formaldehyde at room temperature. Subsequently, cells were lysed using lysis buffer and sonicated for 30 min. Finally, the sonicated lysate was immuno-precipitated with anti-EZH2, anti-H3K27me3 or anti-IgG. EZH2 forward primers: 5'-TGCACATCCTGACTTCTGTG-3', and reverse primers: 5'- AAGGGCATTCACCAACTCC-3'.

Statistics

SPSS 20.0 software (IBM, Armonk, NY, USA) was used for data analyses. Data were expressed as mean ± standard deviation. Intergroup differences were analyzed by the t-test. $P<0.05$ was considered statistically significant.

Results

Upregulated FBXL19-AS1 in HCC

Compared with adjacent normal tissues, FBXL19-AS1 was upregulated in HCC tissues (Figure 1A). HCC tissues with >5 cm in tumor size had higher level of FBXL19-AS1 relative to those ≤ 5 cm (Figure 1B). Based on tumor staging, HCC patients in stage III-IV presented higher level of FBXL19-AS1 than those in stage I-II (Figure 1C). *In vitro* level of FBXL19-AS1 was upregulated in HCC cell lines relative to that of normal liver cell line (Figure 1D).

Knockdown of FBXL19-AS1 suppressed proliferation, cell cycle progression and induced apoptosis of HCC

Three sh-FBXL19-AS1 vectors were constructed and their transfection efficacies were verified

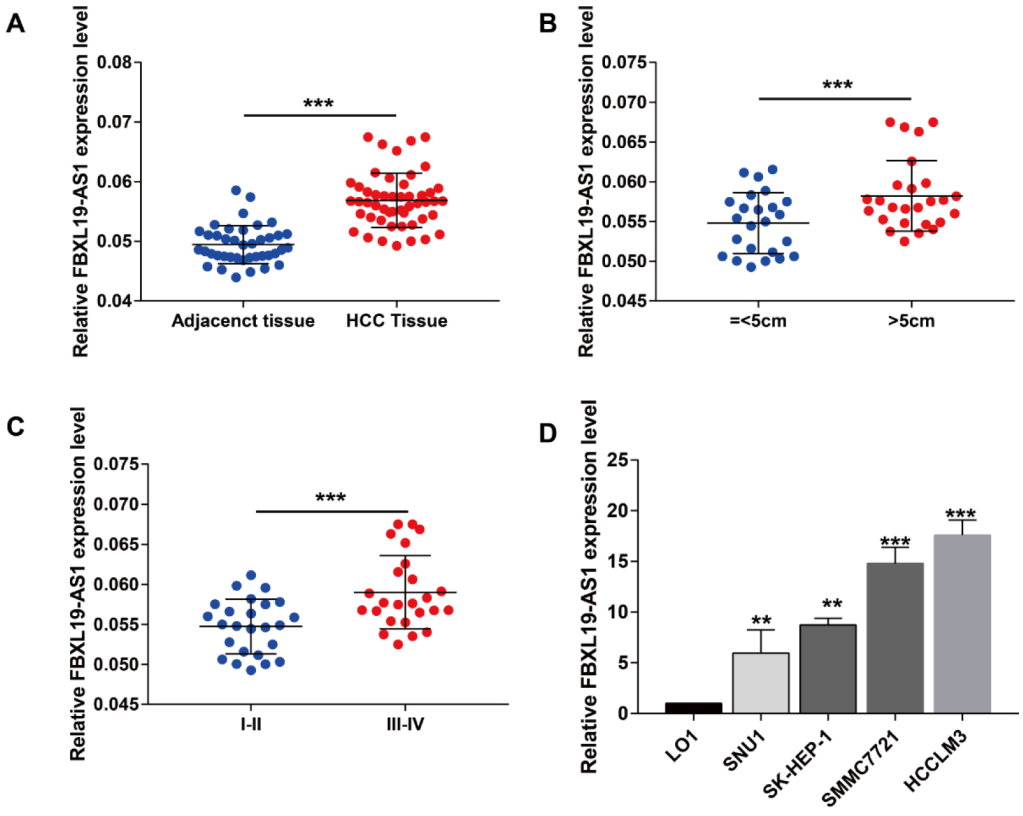

Figure 1. Upregulated FBXL19-AS1 in HCC. **A:** Relative level of FBXL19-AS1 in adjacent normal tissues and HCC tissues. **B:** Relative level of FBXL19-AS1 in HCC tissues >5 cm and ≤ 5 cm in tumor size. **C:** Relative level of FBXL19-AS1 in HCC patients with stage III-IV and stage I-II. **D:** Relative level of FBXL19-AS1 in normal liver cell line and HCC cell lines. **p<0.01, ***p<0.001.

in SMMC7721 and HCCLM3 cells. QRT-PCR data showed that transfection of sh-FBXL19-AS1 2# and sh-FBXL19-AS1 3# markedly downregulated FBXL19-AS1 level in HCC cells (Figure 2A). At 48, 72 and 96 h, transfection of sh-FBXL19-AS1 2# and sh-FBXL19-AS1 3# decreased the viability in HCC cells (Figure 2B, 2C). Besides, the apoptotic rate was elevated by knockdown of FBXL19-AS1 (Figure 2D). After transfection of sh-FBXL19-AS1 2# and sh-FBXL19-AS1 3#, cell ratio in G0/G1 phase markedly increased, suggesting the arrested cell cycle progression (Figure 2E). EdU assay revealed that

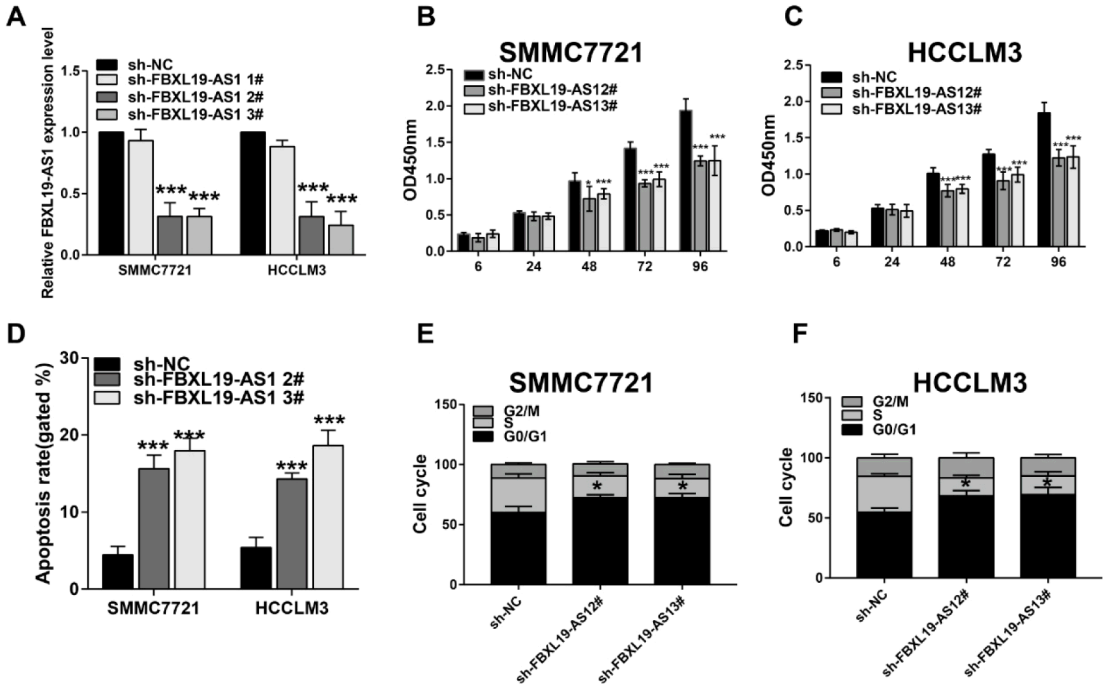

Figure 2. Knockdown of FBXL19-AS1 suppressed proliferation, cell cycle progression and induced apoptosis of HCC. **A:** Transfection efficacies of sh-FBXL19-AS1 1#, sh-FBXL19-AS1 2# and sh-FBXL19-AS1 3# in SMMC7721 and HCCLM3 cells. **B:** CCK-8 assay showed viability in SMMC7721 cells transfected with sh-NC, sh-FBXL19-AS1 2# or sh-FBXL19-AS1 3#. **C:** CCK-8 assay showed viability in HCCLM3 cells transfected with sh-NC, sh-FBXL19-AS1 2# or sh-FBXL19-AS1 3#. **D:** Apoptotic rate in SMMC7721 and HCCLM3 cells transfected with sh-NC, sh-FBXL19-AS1 2# or sh-FBXL19-AS1 3#. **E:** Cell cycle progression in SMMC7721 cells transfected with sh-NC, sh-FBXL19-AS1 2# or sh-FBXL19-AS1 3#. **F:** Cell cycle progression in HCCLM3 cells transfected with sh-NC, sh-FBXL19-AS1 2# or sh-FBXL19-AS1 3#. ***p<0.001.

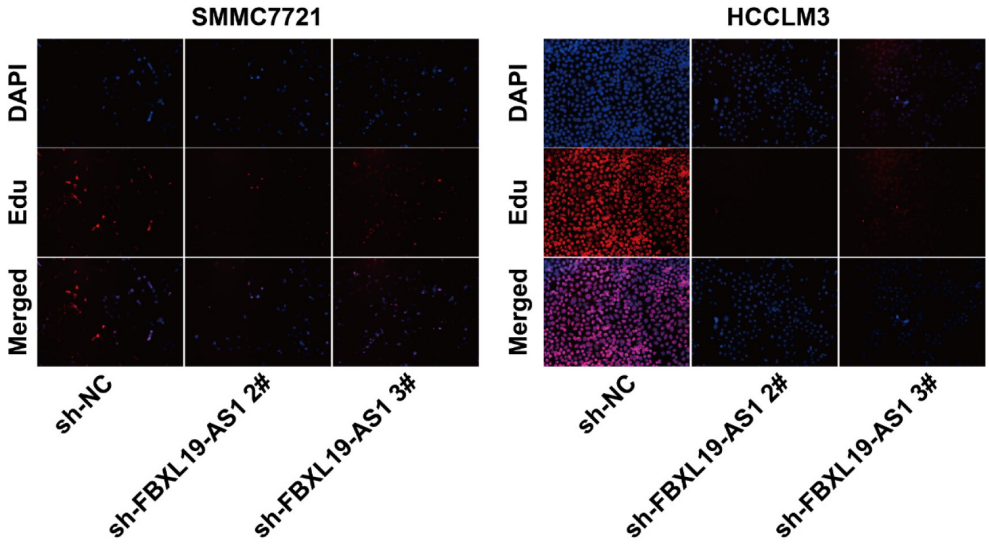

Figure 3. Knockdown of FBXL19-AS1 suppressed the proliferative ability of HCC. EdU assay showed DAPI-labeled (blue), EdU-labeled (red) and merged cells in SMMC7721 and HCCLM3 cells transfected with sh-NC, sh-FBXL19-AS1 2# or sh-FBXL19-AS1 3#.

transfection of sh-FBXL19-AS1 2# or sh-FBXL19-AS1 3# in SMMC7721 and HCCLM3 cells reduced the number of EdU-positive cells, suggesting the attenuated proliferative ability (Figure 3).

FBXL19-AS1 downregulated KLF2 through recruiting EZH2

KLF2 level was found to be upregulated in HCC cells transfected with sh-FBXL19-AS1 2# or sh-FBXL19-AS1 3# (Figure 4A,4B). Through subcellular distribution analysis, FBXL19-AS1 was identified to be mainly distributed in the nucleus of HCC cells (Figure 4C). Moreover, RIP assay revealed higher enrichment of FBXL19-AS1 in anti-EZH2 and anti-SUZ12 relative to anti-IgG (Figure 4D). Transfection of sh-EZH2 remarkably downregulated EZH2 level and upregulated KLF2 level in HCCLM3 cells (Figure 4E). Furthermore, transfection of sh-FBXL19-AS1 2# decreased the recruitment ability of EZH2 on KLF2, indicating that KLF2 level was regulated by FBXL19-AS1 through recruiting EZH2 (Figure 4F).

Knockdown of KLF2 reversed the regulatory effect of FBXL19-AS1 on HCC proliferation

Transfection of sh-KLF2 markedly downregulated KLF2 level in HCCLM3 cells, demonstrating the pronounced transfection efficacy (Figure 5A). Notably, the decreased number of EdU-positive HCCLM3 cells transfected with sh-FBXL19-AS1 2# was partially reversed after co-transfection of sh-KLF2 (Figure 5B). Hence, it is believed that FBXL19-AS1 influenced the proliferative ability of HCC by regulating KLF2.

Discussion

HCC is a primary liver cancer with high mortality. The incidence of HCC is particularly high in Asia, Africa and Southern Europe [16]. Several risk factors for HCC have already been confirmed, including hepatitis B or hepatitis C virus infection and alcohol abuse. The molecular mechanism underlying the pathogenesis and metastasis of HCC is poorly explored [17]. It is of significance to explore

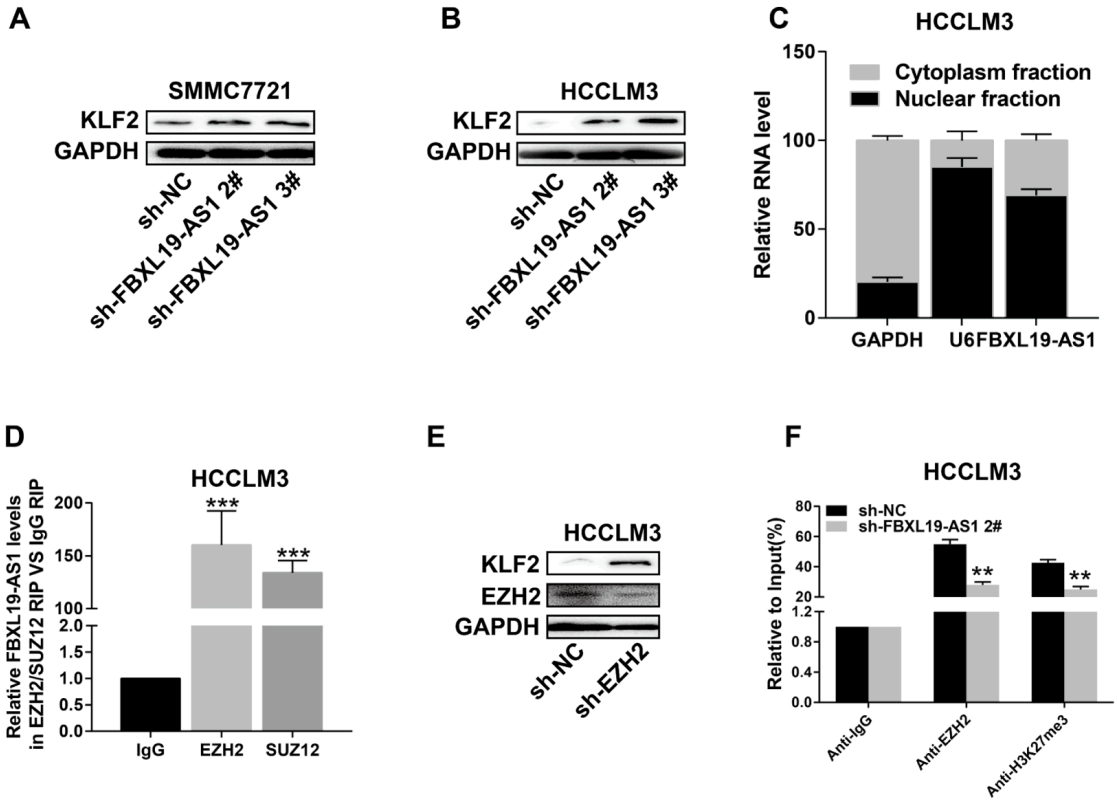

Figure 4. FBXL19-AS1 downregulated KLF2 through recruiting EZH2. **A:** Protein level of KLF2 in SMMC7721 cells transfected with sh-NC, sh-FBXL19-AS1 2# or sh-FBXL19-AS1 3#. **B:** Protein level of KLF2 in HCCLM3 cells transfected with sh-NC, sh-FBXL19-AS1 2# or sh-FBXL19-AS1 3#. **C:** Subcellular distribution of FBXL19-AS1 in the cytoplasm fraction and nuclear fraction. GAPDH and U6 served as cytoplasmic and nuclear internal reference, respectively. **D:** RIP assay showed enrichment of FBXL19-AS1 in anti-IgG, anti-EZH2 and anti-SUZ12. **E:** Protein levels of KLF2 and EZH2 in HCCLM3 cells transfected with sh-NC or sh-EZH2. **F:** ChIP assay showed relative immunoprecipitant of HCCLM3 transfected with sh-NC or sh-FBXL19-AS1 2# in anti-IgG, anti-EZH2 and anti-H3K27me3. **p<0.01, ***p<0.001.

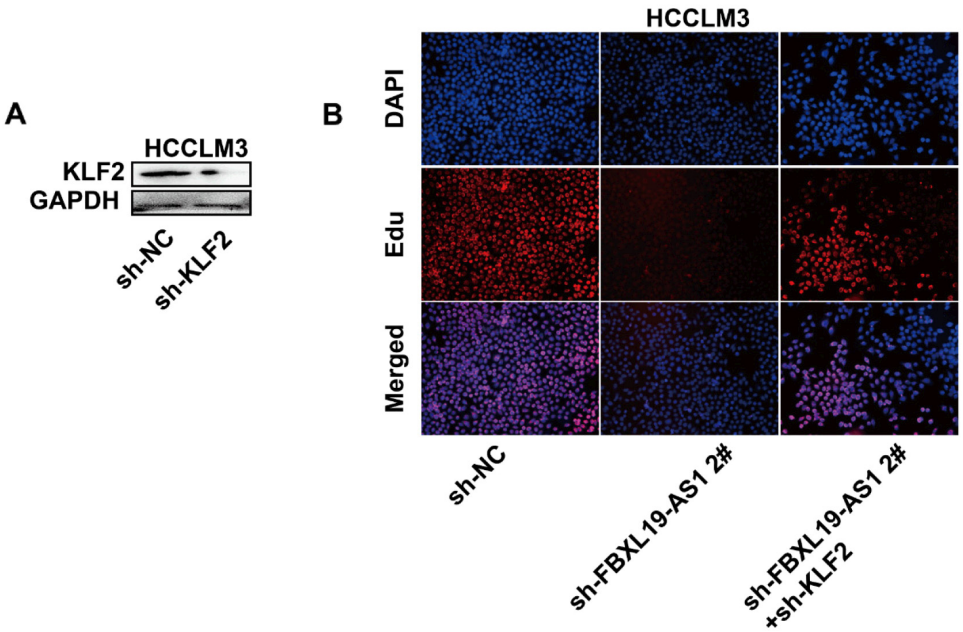

Figure 5. Knockdown of KLF2 reversed the regulatory effect of FBXL19-AS1 on HCC proliferation. **A:** Transfection efficacy of sh-KLF2 in HCCLM3 cells. **B:** EdU assay showed DAPI-labeled (blue), EdU-labeled (red) and merged cells in HCCLM3 cells transfected with sh-NC, sh-FBXL19-AS1 2# or sh-FBXL19-AS1 2#+sh-KLF2.

the etiology and pathogenesis of HCC, thus improving the therapeutic efficacy.

In recent years, lncRNAs are proved to participate in the occurrence and progression of tumors at transcriptional or post-transcriptional level [18]. Functionally, lncRNAs regulate mRNA precursor modification according to the principle of base pairing or interact with proteins and miRNAs to mediate gene expressions. Besides, lncRNAs are involved in epigenetic modification through recruiting chromatin-modifying enzyme complexes to the targeted regions [19,20]. Multiple lncRNAs are abnormally expressed in HCC. These lncRNAs could influence the progression of HCC by regulating corresponding target genes [21]. In this study, FBXL19-AS1 was upregulated in HCC tissues. Furthermore, FBXL19-AS1 accelerated the proliferative ability and cell cycle progression, but inhibited apoptosis of HCC cells.

KLF2 is expressed on embryonic day 14. A previous experiment showed that endothelial-specific KLF2 knockout mice die of bleeding and high-output heart failure due to loss of vascular integrity [22]. Exposure to laminar shear stress stimulates glomerular endothelial cells to activate the ERK5 signaling pathway, upregulate KLF2 and its downstream genes eNOS, THBD and ET-1 [23]. It is indicated that KLF2 exerts a protective role on endothelial function. KLF2 is implicated to be downregulated in a variety of tumors [24]. Chen et al [25] illustrated the potentiation of treatment efficacy against colon cancer *via* elevating KLF2 expression in tumor vascular endothelial cells. In this study, KLF2 was negatively regulated by FBXL19-AS1 in HCC. Knockdown of KLF2 reversed the regulatory effect of FBXL19-AS1 on the proliferative ability of HCC cells. To sum up, FBXL19-AS1 aggravated the progression of HCC via interacting with KLF2.

Conclusions

LncRNA FBXL19-AS1 accelerates the proliferative ability, cell cycle progression and suppresses apoptosis of tumor cells through interacting with KLF2, thus aggravating the progression of HCC.

Conflict of interests

The authors declare no conflict of interests.

References

1. Zhou P, Cheng Y, Liu F, Wu K, Qiu W, Wang S. Tanshindiol-C suppresses in vitro and in vivo hepatocellular cancer cell growth by inducing mitochondrial-mediated apoptosis, cell cycle arrest, inhibition of angiogenesis and modulation of key tumor-suppressive miRNAs. J BUON 2019;24:622-7.

2. Cheung TT, Han HS, She WH et al. The Asia Pacific Consensus Statement on Laparoscopic Liver Resection for Hepatocellular Carcinoma: A Report from the 7th Asia-Pacific Primary Liver Cancer Expert Meeting Held in Hong Kong. Liver Cancer 2018;7:28-39.
3. Wu J, Jiang ZM, Xie Y et al. miR-218 suppresses the growth of hepatocellular carcinoma by inhibiting the expression of proto-oncogene Bmi-1. J BUON 2018;23:604-10.
4. Liu Z, Zhang Y, Xu Z. UNC119 promotes the growth and migration of hepatocellular carcinoma via Wnt/beta/catenin and TGF/beta-EMT signaling pathways. J BUON 2018;23:188-92.
5. Costa FF. Non-coding RNAs: new players in eukaryotic biology. Gene 2005;357:83-94.
6. Okazaki Y, Furuno M, Kasukawa T et al. Analysis of the mouse transcriptome based on functional annotation of 60,770 full-length cDNAs. Nature 2002;420:563-73.
7. Kretz M, Siprashvili Z, Chu C et al. Control of somatic tissue differentiation by the long non-coding RNA TINCR. Nature 2013;493:231-5.
8. Hu J, Qian Y, Peng L et al. Long Noncoding RNA EGFR-AS1 Promotes Cell Proliferation by Increasing EGFR mRNA Stability in Gastric Cancer. Cell Physiol Biochem 2018;49:322-34.
9. Zhu Y, Dai B, Zhang H, Shi G, Shen Y, Ye D. Long non-coding RNA LOC572558 inhibits bladder cancer cell proliferation and tumor growth by regulating the AKT-MDM2-p53 signaling axis. Cancer Lett 2016;380:369-74.
10. Park SM, Choi EY, Bae DH, Sohn HA, Kim SY, Kim YJ. The LncRNA EPEL Promotes Lung Cancer Cell Proliferation Through E2F Target Activation. Cell Physiol Biochem 2018;45:1270-83.
11. Zhang L, Yang F, Yuan JH et al. Epigenetic activation of the MiR-200 family contributes to H19-mediated metastasis suppression in hepatocellular carcinoma. Carcinogenesis 2013;34:577-86.
12. Shen B, Yuan Y, Zhang Y et al. Long non-coding RNA FBXL19-AS1 plays oncogenic role in colorectal cancer by sponging miR-203. Biochem Biophys Res Commun 2017;488:67-73.
13. Nie FQ, Sun M, Yang JS et al. Long noncoding RNA ANRIL promotes non-small cell lung cancer cell proliferation and inhibits apoptosis by silencing KLF2 and P21 expression. Mol Cancer Ther 2015;14:268-77.
14. Das H, Kumar A, Lin Z et al. Kruppel-like factor 2 (KLF2) regulates proinflammatory activation of monocytes. Proc Natl Acad Sci U S A 2006;103:6653-8.
15. Lian Y, Yan C, Xu H et al. A Novel lncRNA, LINC00460, Affects Cell Proliferation and Apoptosis by Regulating KLF2 and CUL4A Expression in Colorectal Cancer. Mol Ther Nucleic Acids 2018;12:684-97.
16. Torre LA, Bray F, Siegel RL, Ferlay J, Lortet-Tieulent J, Jemal A. Global cancer statistics, 2012. CA Cancer J Clin 2015;65:87-108.
17. Wei W, Du C, Lv J et al. Blocking A2B adenosine receptor alleviates pathogenesis of experimental autoimmune encephalomyelitis via inhibition of IL-6 production and Th17 differentiation. J Immunol 2013;190:138-46.
18. Sheng L, Ye L, Zhang D, Cawthorn WP, Xu B. New Insights Into the Long Non-coding RNA SRA: Physiological Functions and Mechanisms of Action. Front Med (Lausanne) 2018;5:244.
19. Tsai MC, Manor O, Wan Y et al. Long noncoding RNA as modular scaffold of histone modification complexes. Science 2010;329:689-93.
20. Tripathi V, Ellis JD, Shen Z et al. The nuclear-retained noncoding RNA MALAT1 regulates alternative splicing by modulating SR splicing factor phosphorylation. Mol Cell 2010;39:925-38.
21. Li C, Chen J, Zhang K, Feng B, Wang R, Chen L. Progress and Prospects of Long Noncoding RNAs (lncRNAs) in Hepatocellular Carcinoma. Cell Physiol Biochem 2015;36:423-34.
22. Lee JS, Yu Q, Shin JT et al. Klf2 is an essential regulator of vascular hemodynamic forces in vivo. Dev Cell 2006;11:845-57.
23. Slater SC, Ramnath RD, Uttridge K et al. Chronic exposure to laminar shear stress induces Kruppel-like factor 2 in glomerular endothelial cells and modulates interactions with co-cultured podocytes. Int J Biochem Cell Biol 2012;44:1482-90.
24. Taniguchi H, Jacinto FV, Villanueva A et al. Silencing of Kruppel-like factor 2 by the histone methyltransferase EZH2 in human cancer. Oncogene 2012;31:1988-94.
25. Chen S, Zhang YM, Zhang YG, Jia J, Zhu RW. Potentiation of treatment efficacy against colon cancer of dopamine via elevating KLF2 expression in tumor vascular endothelial cells. Eur Rev Med Pharmacol Sci 2017;21:4860-6.